Surface location error for helical mills

D. Bachrathy[1], M. Homer[2], T. Insperger[1], G. Stépán[1]

[1]Department of Applied Mechanics, Budapest University of Technology and Economics, Budapest, Hungary
[2]Department of Engineering Mathematics, University of Bristol, Bristol, UK

Abstract
Stability and surface location error are investigated numerically for milling operations with a helical tool. A detailed mechanical model is derived that includes both surface regeneration and the helical teeth of the tool. The governing delay-differential equation is analyzed by a modified version of the semi-discretization method. The surface location error is predicted based on the (stable) forced motion of the tool for different axial depths of cut. It is shown that the surface location error varies periodically along the axial direction due to the helical teeth. The relation of the maximum surface location error, the surface waviness and the surface roughness is explored.

Keywords:
Helical mills, surface location error, time delay, stability

1 INTRODUCTION

Machine tool vibration is one of the most important problems that faces the machinist. Undesired vibrations during machining, often called machine tool chatter, shorten the lifetime of the tool and result in unacceptable surface quality. Recently, the research interest has focused on the determination of the chatter-free technological parameters in order to check the surface quality for stable operations.

While in milling processes it is essential to use stable machining, the surface properties are also very important for finishing. Efficient technical parameters for stable cutting can be chosen from the stability charts, but in most cases, forced vibrations still occur at these parameters. Most studies in the literature of machine tool chatter consider straight fluted tool models [1,2,3,4], and few articles use models to describe the effects of the helix angle of the tool [5]. The surface properties are usually determined by a straight fluted tool model [3,4], even though machine tools typically have helical edges; see [8] for geometric description of the surface in a helical tool model.

The goal of this paper is to predict the surface properties by means of a helical tool model.

2 MODEL

In our analysis, a 2 DoF flexible tool and rigid work-piece model was used (Fig. 1.), because the first modal frequencies in the x and y directions are the lowest and most important due to the small damping of the machine tool structure.

In finishing operations, only the stable process is acceptable, which can be determined by a linear stability calculation. Thus, the cutting force $\mathbf{F}_j$ of the j th tooth is approximated as a linear function of the chip thickness h_j at the stationary cutting, and the ratio of the tangential cutting force component $F_j^{\mathrm{t}}(t)$ and the radial one $F_j^{\mathrm{r}}(t)$ is supposed to be constant:

$$F_j^{\mathrm{t}}(t) = w k_{\mathrm{t}} h_j(t), \quad \frac{F_j^{\mathrm{t}}(t)}{F_j^{\mathrm{r}}(t)} = \mathrm{const} = k_{\mathrm{r}}, \tag{1}$$

where w is the axial immersion, k_r and k_t are so called cutting coefficients. The chip thickness comprises two parts, the static and the dynamic chip thicknesses. The static part is generated by the constant feed motion v, while the vibration of the tool described by the general coordinate vector $\mathbf{q}=[\mathrm{x\ y}]^{\mathrm{T}}$ generates the dynamic part, so

$$h_j(t) = \left[\sin(\phi_j(t)) \quad \cos(\phi_j(t))\right]\left(\begin{bmatrix}\tau v\\ 0\end{bmatrix} + \mathbf{q}(t) - \mathbf{q}(t-\tau)\right), \tag{2}$$

where $\phi_j(t)$ is the angular position of the jth tooth, $\tau = 2\pi/\Omega Z$ is the time delay, Z is the number of the teeth and Ω is the angular velocity of the tool. This formula already contains the so called regenerative effect, too, with the presence of the time delayed term $\mathbf{q}(t-\tau)$.

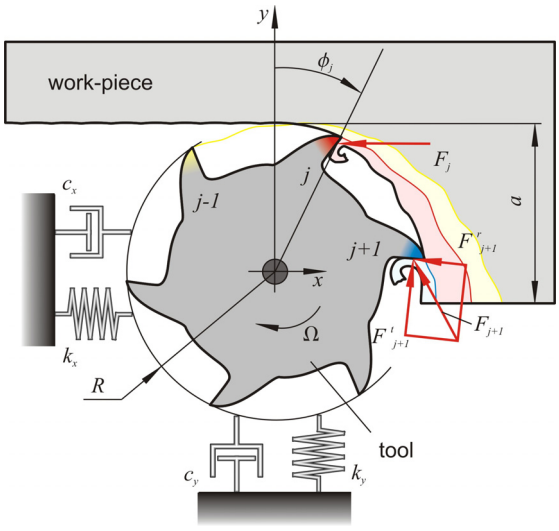

Figure 1: 2DoF model.

From the modal analysis, we know the mass (**M**), the damping (**C**) and the stiffness (**K**) matrices. The governing equation is given by

$$\mathbf{M}\ddot{\mathbf{q}}(t)+\mathbf{C}\dot{\mathbf{q}}(t)+\mathbf{K}\mathbf{q}(t)=\mathbf{W}(t)\left(\begin{bmatrix}\tau v\\0\end{bmatrix}+\mathbf{q}(t)-\mathbf{q}(t-\tau)\right). \quad (3)$$

In the case of a straight edged tool, the directional force coefficient matrix $\mathbf{W}(t)$ can be calculated easily:

$$\mathbf{W}(t)=\sum_{j=0}^{Z-1}\frac{w k_t}{2}g_j\left(\phi_j(t)\right)\mathbf{T}\left(\phi_j(t)\right). \quad (4)$$

The step function g_j shows whether the jth tooth is in contact with the work-piece, or it is not. The projection matrix $\mathbf{T}$ is given by

$$\begin{aligned}
\mathbf{T}_{11}\left(\phi_j(t)\right)&=-\sin\left(2\phi_j(t)\right)-k_r+k_r\cos\left(2\phi_j(t)\right)\\
\mathbf{T}_{12}\left(\phi_j(t)\right)&=-1-\cos\left(2\phi_j(t)\right)-k_r\sin\left(2\phi_j(t)\right)\\
\mathbf{T}_{21}\left(\phi_j(t)\right)&=1-\cos\left(2\phi_j(t)\right)-k_r\sin\left(2\phi_j(t)\right)\\
\mathbf{T}_{22}\left(\phi_j(t)\right)&=\sin\left(2\phi_j(t)\right)-k_r-k_r\cos\left(2\phi_j(t)\right)
\end{aligned} \quad (5)$$

2.1 Helical edged tool

In our model in Fig. 2, the current angular position of the edge also depends on the axial coordinate of the tool z.

$$\phi_j(z,t)=t\Omega+j\frac{2\pi}{Z}-\frac{2\pi z}{p}, \quad (6)$$

where p is the helix pitch.

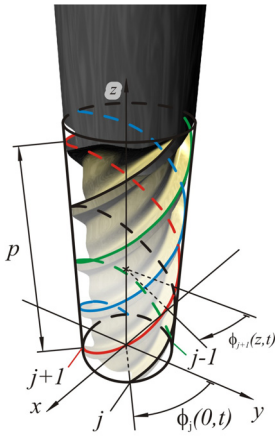

Figure 2: Geometry of a helical edged tool.

The system of the helical tool model can be described with the same governing equation as (3), but we must use a different directional force coefficient matrix, which is given by

$$\widetilde{\mathbf{W}}(t)=\sum_{j=0}^{Z-1}\widetilde{\mathbf{W}}_j(t)=\sum_{j=0}^{Z-1}\int_{z=0}^{w}\frac{k_t}{2}g_j\left(\phi_j(z,t)\right)\mathbf{T}\left(\phi_j(z,t)\right)dz. \quad (7)$$

Fig. 3 shows that if the axial immersion is large enough then the directional force coefficient matrix in (7) can be separated into two parts:

$$\widetilde{\mathbf{W}}(t)=N_{\text{full}}\overline{\mathbf{W}}+\sum_{j=0}^{Z-1}\mathbf{W}_j(t). \quad (8)$$

where $N_{\text{full}}=\text{int}(wZ/p)$.

The first part contains those sections where the integration is made along full periods (p/Z). This part is constant in time:

$$\overline{\mathbf{W}}=\int_{\phi_{\text{in}}}^{\phi_{\text{out}}}\frac{k_t p}{4\pi}\mathbf{T}\left(\phi_j(z,t)\right)d\phi. \quad (9)$$

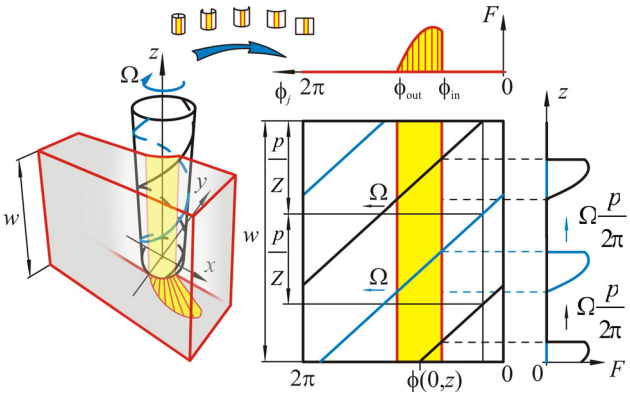

Figure 3: Helix pitch and angular position of the edge as a function of the coordinate z.

The second part contains the remainder of the integration, which is time dependent:

$$\mathbf{W}_j(t)=\int_{a_j(t)}^{b_j(t)}\frac{k_t p}{4\pi}\mathbf{T}\left(\phi_j(z,t)\right)d\phi. \quad (10)$$

The limits $a_j(t),b_j(t)$ of the integration can be determined from the systematic scheduling of entry and exit angles, so the directional force coefficient matrix can be calculated analytically [6]. The directional force coefficient matrix is time independent if the $\mathbf{W}_j$ is zero, so we integrate along full periods only. In this case

$$w=k\frac{p}{Z},\quad k\in\mathbb{N}. \quad (11)$$

This case is represented in Fig. 4 by the straight-lines.

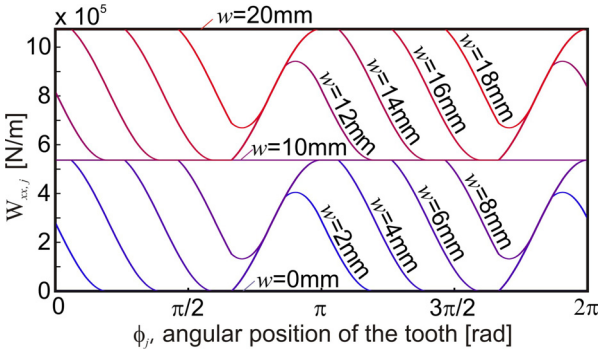

Figure 4: Function of the xx component of the directional force coefficient matrix in different axial immersion (w). p/Z=10mm

The governing equation (3) can be separated into two parts by using the new variables $\mathbf{x}$ and $\boldsymbol{\xi}$.

$$\mathbf{q}(t)=\mathbf{x}(t)+\boldsymbol{\xi}(t)=\begin{bmatrix}x(t)\\y(t)\end{bmatrix}+\begin{bmatrix}\xi(t)\\\eta(t)\end{bmatrix}, \quad (12)$$

such that forced motion $\mathbf{x}(t)$ satisfies

$$\mathbf{M}\ddot{\mathbf{x}}(t)+\mathbf{C}\dot{\mathbf{x}}(t)+\mathbf{K}\mathbf{x}(t)=\widetilde{\mathbf{W}}(t)\begin{bmatrix}\tau v\\0\end{bmatrix}, \quad (13)$$

where the right-hand-side contains the time function of the cutting force.

Substituting (12) and (13) into (3) we get the delayed parametrically forced part of the governing equation.

$$\mathbf{M}\ddot{\boldsymbol{\xi}}(t)+\mathbf{C}\dot{\boldsymbol{\xi}}(t)+\left(\mathbf{K}-\widetilde{\mathbf{W}}(t)\right)\boldsymbol{\xi}(t)=-\widetilde{\mathbf{W}}(t)\boldsymbol{\xi}(t-\tau), \quad (14)$$

which describes the stability of the tool motion. If it is unstable, the tool vibration amplitude tends to infinity and there is no need to calculate the surface, this is already unacceptable. When the trivial solution $\boldsymbol{\xi}(t)\equiv\mathbf{0}$ of (14) is stable, the particular motion of the tool centre is given by the solution of the forced motion (13). This always has a

periodic solution because of the small damping. By using this solution, we can compute the motion of the teeth, which generates the surface after the settled transient motion.

The parameter domains of stable cutting were calculated from (14) using the semi-discretization method, which is described in detail in [6,7].

3 SURFACE

To be able to calculate the general solution, we approximate the cutting force by its Fourier series. During the calculations, the first 25 terms were used ($N_F=25$).

$$\tilde{\mathbf{W}}(t)\begin{bmatrix}\tau v\\ 0\end{bmatrix} \cong \mathbf{a}_0 + \sum_{j=1}^{N_F}\mathbf{a}_j \cos\left(\frac{2\pi j t}{\tau}\right) + \mathbf{b}_j \sin\left(\frac{2\pi j t}{\tau}\right). \quad (15)$$

The particular solution of the tool-centre vibration is also given by a series of trigonometric functions

$$\mathbf{x}(t) \cong \mathbf{c}_0 + \sum_{j=1}^{N_F}\mathbf{c}_j \cos\left(\frac{2\pi j t}{\tau}\right) + \mathbf{d}_j \sin\left(\frac{2\pi j t}{\tau}\right). \quad (16)$$

The coefficients $\mathbf{c}$ and $\mathbf{d}$ can be determined from

$$\begin{bmatrix}\mathbf{c}_j\\ \mathbf{d}_j\end{bmatrix} = \begin{bmatrix}\mathbf{K}-\left(\frac{2\pi j}{\tau}\right)^2\mathbf{M} & \mathbf{C}\left(\frac{2\pi j}{\tau}\right)\\ -\mathbf{C}\left(\frac{2\pi j}{\tau}\right) & \mathbf{K}-\left(\frac{2\pi j}{\tau}\right)^2\mathbf{M}\end{bmatrix}^{-1}\begin{bmatrix}\mathbf{a}_j\\ \mathbf{b}j\end{bmatrix}. \quad (17)$$

Using the solution $\mathbf{x}(t)$, the motion of the jth cutting edge $\mathbf{e}_j(z,t)$ can be described by superposing this vibration onto the cylindrical rotation; see Fig.5. The cylinder is created by the edge of the rigid tool.

$$\mathbf{e}_j(z,t) = \begin{bmatrix}x(t)\\ y(t)\end{bmatrix} + \begin{bmatrix}R\cos(\phi_j(z,t))\\ R\sin(\phi_j(z,t))\end{bmatrix}, \quad (18)$$

where R is the radius of the tool and ϕ_j comes from (6).

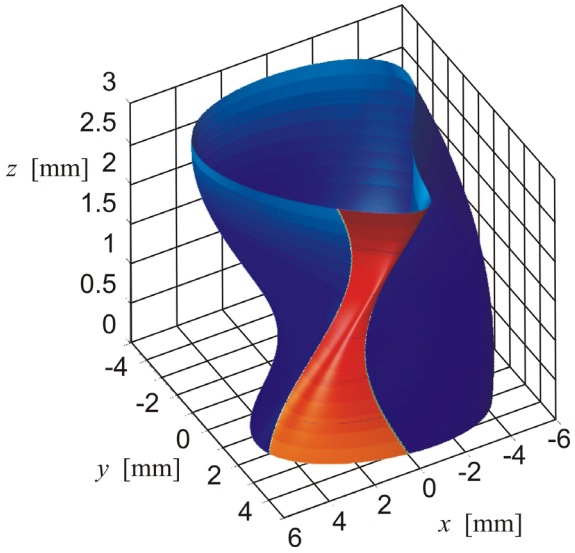

Figure 5: Path of the helical edges $\mathbf{e}(z,t)$. Red surface denotes the cutting period, blue surface denotes the non-cutting period.

During the milling process, each tooth create a single surface segment $\mathbf{s}(z,t)$ in every revolution. The whole surface is formed by these surface segments (see Fig.6.). Every surface segment is the same because we neglect the transient motion of the tool. The surface properties can be described by a single surface segment, which can be determined by the motion $\mathbf{e}(z,t)$ of any edge relative to the work-piece:

$$\mathbf{s}(z,t) = \mathbf{e}(z,t(z)) + \begin{bmatrix}vt\\ 0\end{bmatrix} \quad t \in \left[t_{start}(z), t_{end}(z)\right]. \quad (19)$$

We have to determine the entering and exiting time instants $t_{start}(z), t_{end}(z)$ at a certain height z when the cutting edge just touches the boundary of the surface segment of the work-piece. These can be calculated from

$$\mathbf{e}(z,t_{\text{start},}(z)) + \begin{bmatrix}vt_{start}(z)\\ 0\end{bmatrix} + \begin{bmatrix}\tau v\\ 0\end{bmatrix} = \mathbf{e}(z,t_{\text{end}}(z)) + \begin{bmatrix}vt_{end}(z)\\ 0\end{bmatrix}. \quad (20)$$

3.1 Surface properties

In case of the straight fluted tool, two surface parameters are commonly used. First is the surface roughness μ given by

$$\mu = \max_t\left(\mathbf{s}_y(t)\right) - \min_t\left(\mathbf{s}_y(t)\right). \quad (21)$$

Second is the surface location error SLE, which is an offset error. It is the distance between the desired surface and the machined surface. SLE can be calculated by

$$SLE = \max_t\left(\mathbf{s}_y(t)\right) - R. \quad (22)$$

In the helical tool model, the surface roughness and the surface location error are the functions of the axial coordinate z, that is we have the corresponding functions μ(z), SLE(z). It is more convenient, though, to describe surface properties by a single scalar quantity. In practice the surface quality is described by the largest difference between the points of the surface. Using a tool with a helical edge, there are two different deflections. The first is in the feed direction x, which is similar to surface roughness at the straight fluted tool model. The second is in the z direction due to the varying $SLE(z)$. This error is caused only by the helical edge, and hence it is always zero in the case of a straight fluted tool.

It can be seen from (18) and (6), that the surface is changing periodically along the z coordinate, too. The variation of SLE has wavelength p/Z in the direction z. For this reason, the variation of SLE is not really a surface roughness but rather a surface waviness. Consequently, the surface error is separated into two parts. The first is the **surface roughness** μ_x:

$$\mu_x = \max_z(\mu(z)). \quad (23)$$

The second is the **surface waviness** $\tilde{\mu}$, given by

$$\tilde{\mu} = \max_z\left(SLE(z)\right) - \min_z\left(SLE(z)\right). \quad (24)$$

An overall scalar characteristic value of the surface could be the **maximum surface location error** $MSLE$, which is given by

$$MSLE = \max_{z,t}(\mathbf{s}_y(z,t)) - R = \max_z(SLE(z)). \quad (25)$$

If we use straight fluted tool, SLE and $MSLE$ are the same. The three types of surface errors μ_x, $\tilde{\mu}$ and $MSLE$ are represented graphically in Fig. 6.

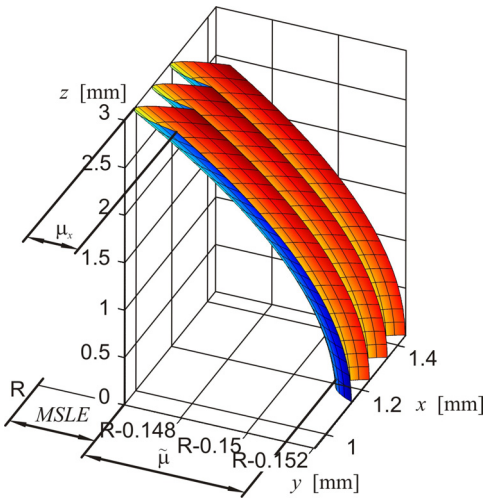

Figure 6: Schematic representation of the surface errors made by helical tool. Three surface segments are shown.

4 MECHANICAL MODEL

4.1 Mechanical parameters

To describe the effect of the technological parameters on the surface quality, we choose a particular machine tool and corresponding work-piece parameters. The machine tool is described by the same modal parameters as used in [3]. These parameters were determined experimentally. The mass (**M**), damping (**C**) and the stiffness (**K**) matrices were determined by a standard impact test procedure of modal analysis:

$$\mathbf{M}=\begin{bmatrix} m_x & 0 \\ 0 & m_y \end{bmatrix}=\begin{bmatrix} 0.01986 & 0 \\ 0 & 0.02008 \end{bmatrix}[kg],$$

$$\mathbf{C}=\begin{bmatrix} c_x & 0 \\ 0 & c_y \end{bmatrix}=\begin{bmatrix} 1.60312 & 0 \\ 0 & 1.155697 \end{bmatrix}\left[\frac{Ns}{m}\right],$$

$$\mathbf{K}=\begin{bmatrix} k_x & 0 \\ 0 & k_y \end{bmatrix}=\begin{bmatrix} 408\,866 & 0 \\ 0 & 413\,445 \end{bmatrix}\left[\frac{N}{m}\right].$$

During the calculations we use tools with a standard radius R=4 mm.

The chosen material of the work-piece is AlMgSi0.5 aluminium alloy, which leads to the numerical values of the tangential cutting coefficient k_t and the non-dimensional force ratio k_r (see [3]):

$$k_{\mathrm{t}}=644\times10^{6}\left[\frac{N}{m^2}\right],\quad k_{\mathrm{r}}=0.368.$$

4.2 Effect of technological parameters

We calculate the machined surface in those technological parameter regions where the cutting process is stable. The surface quality is especially important in finishing operations, where a small radial immersion is typically used. We chose a fixed 5% radial immersion for down milling. Fig. 7(a) shows the surface location error (SLE) and Fig. 7(b) shows the surface roughness (μ) for down-milling over the stability chart for a straight fluted tool. Note, that the surface waviness is always zero for a straight fluted tool.

We can see that there are large offset errors if we are in the vicinity of those angular velocities where the ratio of the natural frequency of the system and the tooth passing frequency is close to an integer. In this case, the tool vibration is close to resonance because the frequencies of higher harmonics of the cutting force are close to the natural frequencies.

In Fig. 8, we calculated the maximum surface location error $MSLE$ and the surfaces roughness μ_x for the same parameters as in Fig. 7, but we changed the helix pitch to 10 mm. We can see that the helix pitch has a great influence on the surface quality. In the case of a constant directional force coefficient matrix, when wZ/p is close to an integer (see (11)), there is no tool vibration, and there is a small but non-zero $MSLE$ due to the constant force. The same phenomenon is experienced for roughness μ_x.

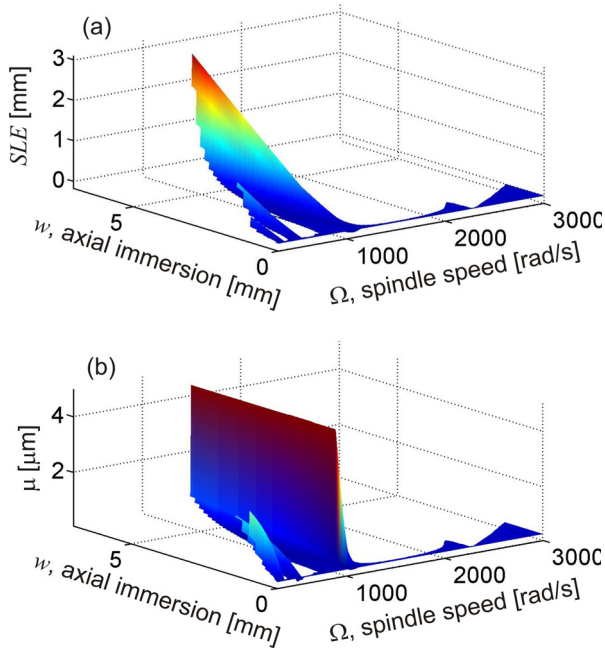

Figure 7: Surface location error SLE (a) and surface roughness μ (b) for down-milling with straight fluted tool. Parameters are Z=4, τv=0.1[mm], p→∞, a/D=0.05.

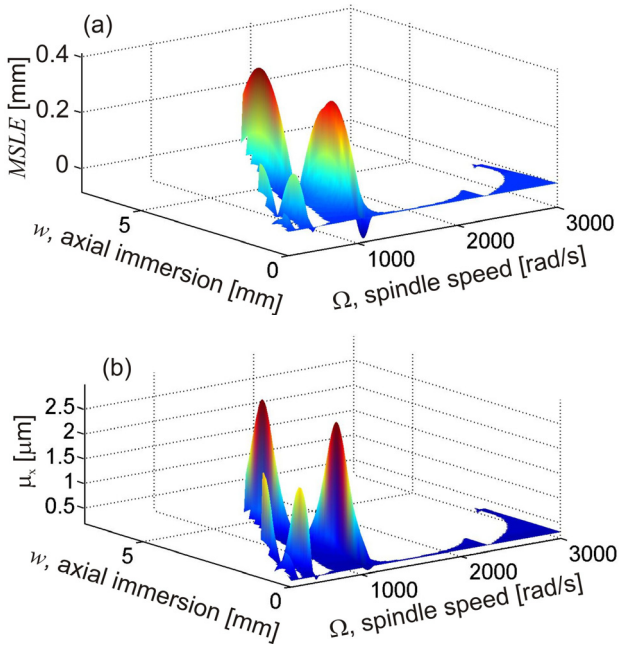

Figure 8: Maximum surface location error (a) and surface roughness (b) for down-milling with helical tool. Parameters are Z=4, τv=0.1[mm], p=10 [mm], a/D=0.05.

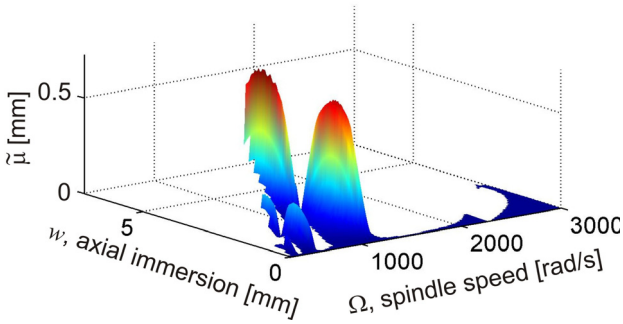

Figure 9: Surface waviness for down-milling with helical tool. Parameters are Z=4, τv=0.1[mm], p=10 [mm], a/D=0.05.

The surface waviness plot is shown in Fig. 9. It can be seen that the surface waviness is in the same order of magnitude as the maximum surface location error. The conclusion is the same: the best surface quality is obtained at the parameter points where wZ/p is close to an integer.

Fig. 8 and 9 show that we can achieve almost the same good surface quality at different parameter values, too. There are as many suitable points in a full helix pitch p/Z as the number of the ratio of the natural frequency and the spindle frequency of the tool. This phenomenon is shown in Fig. 10, where we calculate only MSLE also above the unstable region. The optimal surface quality points are placed along the dotted straight lines.

At these optimal points, the contact period of each edge is an integer multiple of the period of the natural vibration of the tool (see Fig. 11). We can see that the position of the tool centre returns close to the equilibrium after the cutting period partly due to the small damping of the system and partly to the special frequency ratio explained above. This way, significant vibrations cannot emerge, so we get a better surface quality at these points.

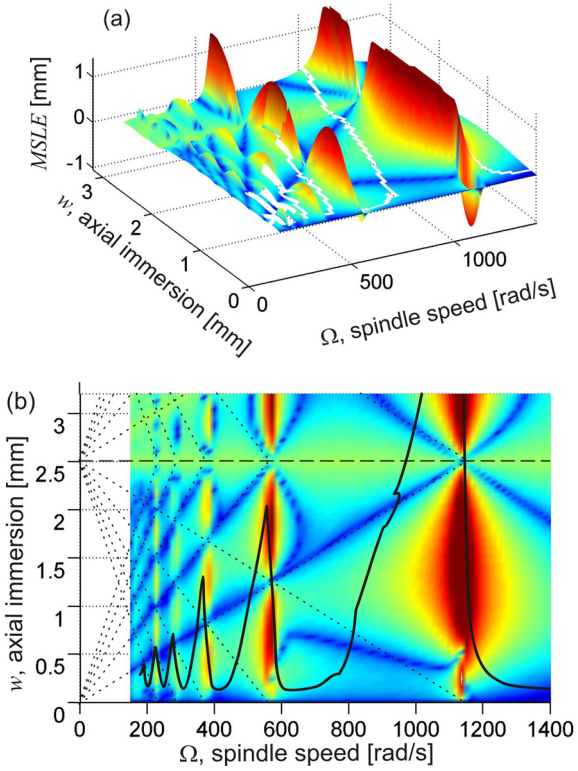

Figure 10: Maximum surface location error (a) and its top view (b). The dashed line denote the p/Z height. Solid line denote the stability boundary. Parameters are Z=4, τv=0.1[mm], p=10 [mm], a/D=0.05.

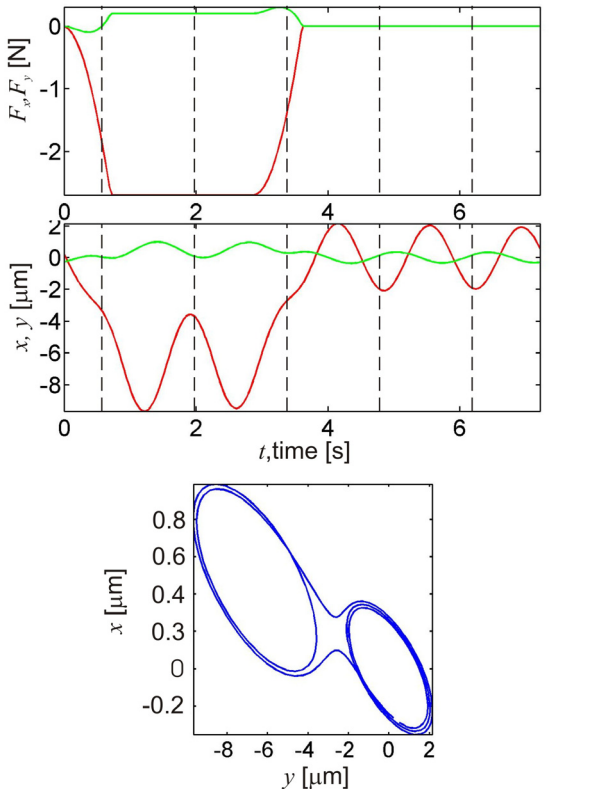

Figure 11: Excitation force (**F**) and the vibration of the tool centre (**x**). Green lines denote the *x* components, red lines denote the *y* components and dash lines denote the period of the natural vibration of the tool. Parameters are Z=1, Ω=888 [rad/s], w=1 [mm], τv=0.05[mm], p=2.5 [mm], a/D=0.1.

5 SUMMARY

In this report, we investigated the effect of the parameters of a helical tool model to predict the surface properties of the machined surface in high-speed milling. First, we determined the governing equation of the tool motion. Then we generated the work-piece surface in the parameter region of stable cutting. New surface parameters like the maximum surface location error $MSLE$, the surface roughness μ_x and the surface waviness $\tilde{\mu}$ were introduced to describe the properties of the surface. The influence of the helix pitch on surface quality was analysed.

Our most important observation was that if we use an appropriate helix pitch, good surface properties can be achieved in the case of resonant angular velocities. We also found the new phenomenon that the appropriate helix pitches are not just those where the directional force coefficient matrix is time independent (so there is constant cutting force in time), but that there are other equally spaced ones between them, where the spacing depends on the angular velocity.

6 ACKNOWLEDGMENTS

This research was supported in part by the János Bolyai Research Scholarship of the Hungarian Academic of Sciences, and by the Hungarian Nation Sciences Foundation under grant no. OTKA F047318 and OTKA T043368.

7 REFERENCES

[1] Gradišek, J., Govekar, E., Grabec, I., Kalveram, M., Weinert, K., Insperger, T., Stépán, G., 2005, On stability prediction for low radial immersion milling, Machine Science and Technology, 9, 117-130.

[2] Mann, B.P., Young, K. A., Schmitz, T.L., Diley, D.N., 2005, Simultaneous Stability and Surface Location Error Predictions in Milling, Journal of Manufacturing Science and Engineering, 127, 446-453.

[3] Insperger, T., Gadišek, J., Kalveram, M., Stépán, G., Weinert, K., Goverkar, E., 2004, Machine tool chatter and surface quality in milling processes, Proceedings of ASME International Mechanical Engineering Conference and Exposition, Anaheim CA, paper no. IMECE2004-59692 (CD-ROM).

[4] Peigné, G., Paris, H., Brissaud, D., 2004, Surface Shape prediction in high speed milling. International Journal of Machine Tool & Manufacture 44, 1567-1576.

[5] Zatarain, M., Munoa, M., Peigné, G., Insperger, T., 2006, Analysis of the influence of mill helix angle on chatter stability, Annals of the CIRP, 55(1), pp. 365-368.

[6] Bachrathy, D., 2006, A study of the milled surface in the dynamics of milling, Msc. Thesis, University of Bristol and Budapest University of Technology and Economics.

[7] Insperger, T., Stépán, G., 2002, Semi-discretization method for delayed systems, International Journal for Numerical Methods in Engineering, 55, 503-518.

[8] Surmann, T., 2006, Geometric model of the surface structure resulting from the dynamic milling process, 9th CRIP International Workshop on Modelling of Machining Operations, 187-192